

Cluster Colour-Magnitude Diagrams

Abstract

The aim of this project was to construct a *colour-magnitude diagram* of one selected open cluster, M67, from just supplied CCD images taken through different filters. CCD images are an invaluable current source of gathering useful scientific information, but in order to maximize its potentially, the data conversion process must be carefully performed.

After photometric data have been properly extracted, it was converted into *standard system* values that finally allowed the construction of the cluster diagram. From its analysis, it was possible to infer an estimation about M67 distance and age. The comparison to published values finally confirmed the validity of the overall executed procedure.

Introduction

This project report will begin with a succinct analysis of the particularities that cluster diagrams show, underlying that just from the morphological analysis of each diagram many essential cluster features can be found out.

Next, it will be presented a detailed description about the complete translation process from raw CCD images to photometry data expressed in an “universal” system. This will include the fundamental topics of *data reduction*, *aperture photometry*, and *standardization*.

Having analyzed the conversion process, its practical application for the open cluster M67 will immediately follow up. It will be described the provided raw CCD images, used software, found peculiarities, obtained data and calculated errors. Some processed images, and a spreadsheet containing all processed data will be attached.

The gathered information will finally allow the construction of the M67 CMD. An analysis of the physical significance of its constituents will be done, resulting in an estimation about M67’s age and distance, as well as expected uncertainties involved. Both estimations will be compared to published data. Lastly, a discussion about the found discrepancies will propose some possible source of errors and the suggested way to avoid them.

1) Why star cluster diagrams are so particular?

Star clusters are groups of stars that appear concentrated in small regions of the sky. As it can be assumed that all star members of a cluster has been formed essentially at the same time from a single primordial cloud of gas and dust, those stars achieve three fundamental common features: (1) they lay at the same distance from us; (2) they have the same age; and (3) they have the same chemical composition. Therefore, stellar clusters become ideal specimens to study the evolution of stars [1].

In order to facilitate any data analysis, a proper graph allows to visualize peculiar features of the sample, such as preferred values, distribution tendencies, prohibited relations, etc. For stellar study, this graph is the classic *Hertzsprung-Rusell* (H-R) diagram, which plots star luminosity (or absolute magnitudes) against their surface temperatures (or spectral types). In particular, if the horizontal variable is expressed as the radiation difference measured from two different wavelengths (the *colour index*), such a diagram is referred to as a *colour-magnitude diagram* (CMD).

Luminosity or absolute magnitude values implies the necessity of knowing the actual distances to stars. On the other hand, surface temperatures or colour indexes can be properly estimated independently of distance. Hence, the practical difficulty for constructing general H-R diagrams is always to know the corresponding distance-dependent values.

For stars lying at the same distance from us (as it certainly is the case for stellar clusters), their apparent magnitudes share a common factor of proportionality with their absolute magnitudes. Therefore, the H-R diagram for a cluster will show the same relative data positions by using distance-dependent absolute magnitudes or the straightforward measured, distance-independent, apparent magnitudes.

This great simplification in the construction of cluster H-R diagrams or cluster CMDs, while still maintaining all their full analysis potentiality, makes them a fundamental tool in both quantitative and qualitative studies of star evolution. The particular morphology of any cluster CMD does reveal a lot about its own characteristics.

2) What features do a cluster CMD reveal?

All stars evolve, some very fast, some very slowly, critically depending on their masses. The more massive a star is, the lesser its lifetime. Mass defines *how long* any star is going to live and the *kind of process* to perform in its final period of life.

But independently of mass, from birth up to 90% of its lifetime, each star evolves in a similar manner. Stars spend most of their lives burning hydrogen slowly in a state of stable equilibrium, and this is the reason why any H-R diagram do not show randomly scattered points over the entire graph, but *mostly concentrated on a band stretching diagonally*. This band is called the Main Sequence, and goes from the upper left (hot, luminous, blue stars) to the lower right (cool, dim, red stars).

When the hydrogen supply in the core of the star is depleted, hydrogen burning is no longer possible. This ends the *main sequence phase* of the star's life, and hence it moves out from its long duration location on the H-R diagram towards the upper right. This new accessed region is known as the Red Giant Branch, and corresponds to the initial stages of the helium burning phase.

Therefore, any considered sample of stars of the same age will necessarily integrate a quite particular stellar diagram. Figure 1 shows a typical CMD of a star cluster, where the massive shorter-lifetime stars have already evolved abandoning their Main Sequence location towards the Red Giant Branch, while many less-massive, long lifetime stars are still placed at the Main Sequence.

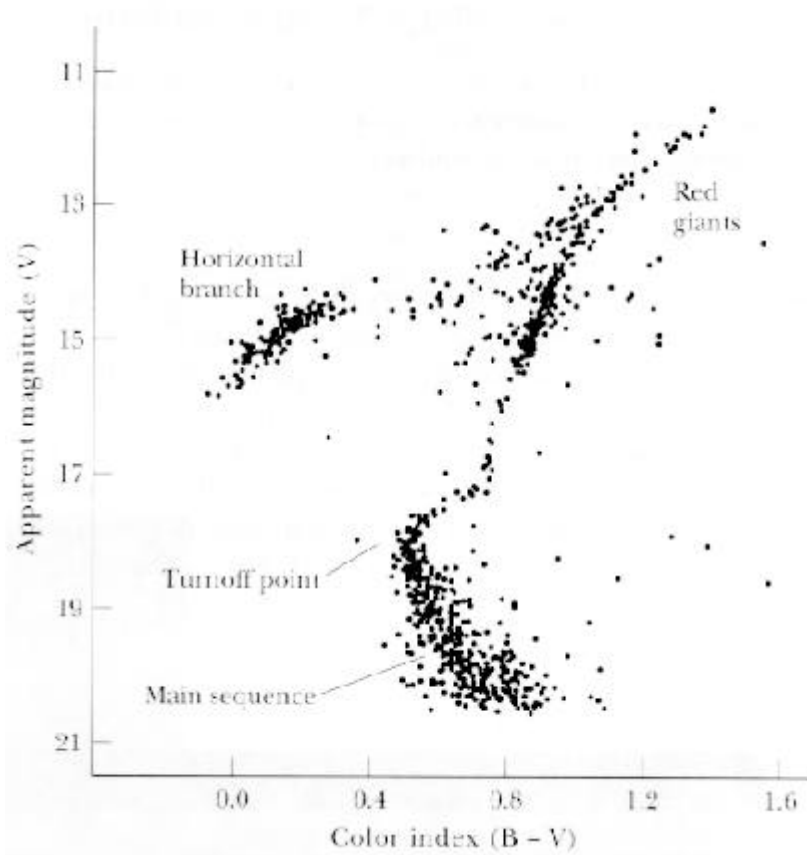


Figure 1
A typical cluster colour-magnitude diagram

Considering star clusters, the point on a H-R diagram or CMD at the top of the still surviving Main Sequence, where the Red Giant Branch seems to begin, is called the *turn-off point*. Knowing its precise location on the diagram gives an important clue to the age of the cluster, as it is possible by comparison to find out the mass (M_{MS}) of stars that have just left the Main Sequence and hence the desired time (t) can be estimated from

$$t \approx (M_{MS})^{-2.5} \quad (1)$$

where both magnitudes are expressed relative to the Sun's mass and lifetime [2].

Another straightforward way to estimate the cluster age is just by comparison the absolute magnitude of the turn-off point to *isochrones* (diagrams plotting absolute magnitude versus Main Sequence lifetime derived from theoretical considerations), as Figure 2 depicts.

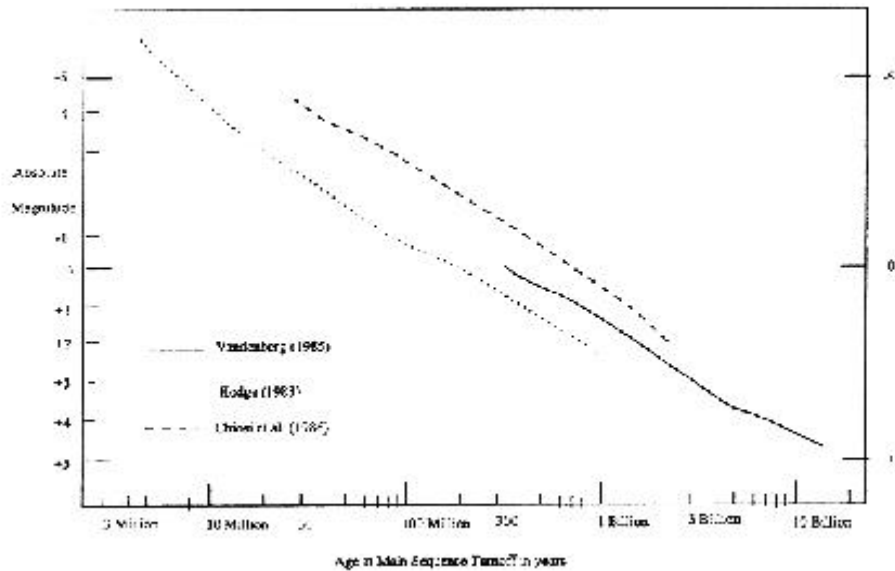


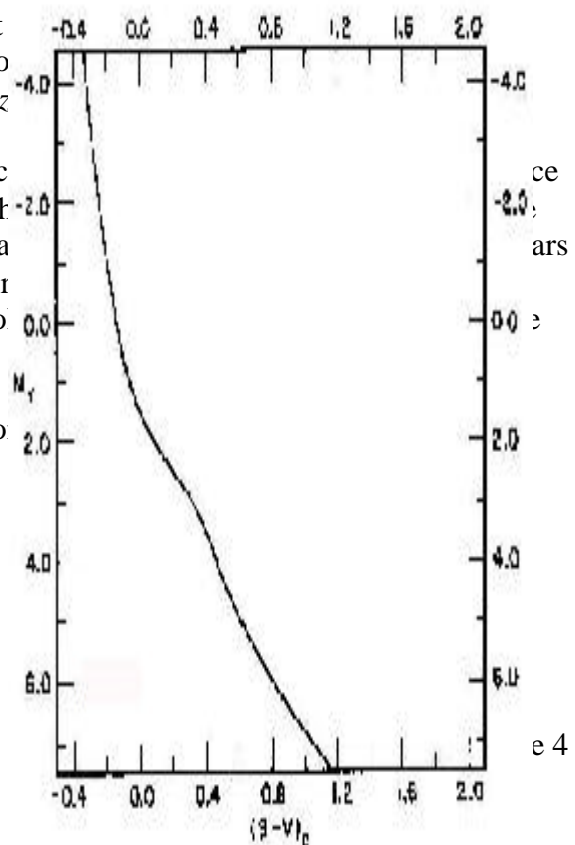
Figure 2

Absolute Visual Magnitude of the main sequence turnoff from Hodge's (1983) calibration, from Van den Berg's (1985) isochrones, and from models from Chiosi et al. (1986)

The distance to the star cluster can be found out Main Sequence CMD (a general graph of absolute magnitude versus colour index values from each graph. The bottom edge of the standard Main Sequence CMD of the cluster. For any star of that common point from the cluster CMD corresponds to the absolute magnitude in the standard diagram.

Therefore, the *distance modulus* ($m - M$) between the cluster (d , in parsecs) can be calculated from

$$d = 10^{\left(\frac{m-M+5}{5}\right)}$$



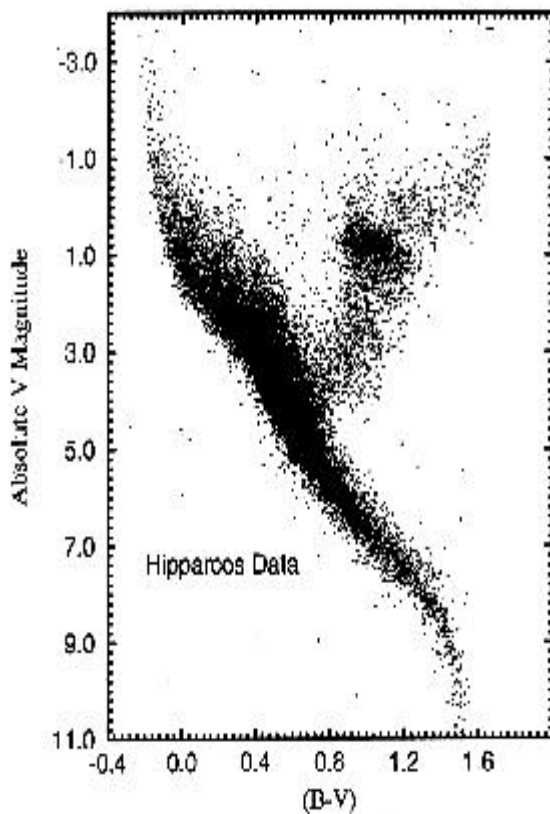


Figure 3
Left: A general CMD of near stars
Right: A sketched CMD only showing the Main Sequence

In finding this preliminary distance from equation (2) it has been omitted the reddening effect of the interstellar dust, which certainly causes a wavelength variable absorption. Although this extinction factor can be considered, thus improving the accuracy of the final “corrected” distance, the achieved improvement is usually negligible compared to the error introduced in the absolute magnitude of the turn-off point by the applied method.

Finally, the construction of a cluster CMD also offers information about its metallicity, that is, an idea about the relative abundance of its constituent elements [3].

3) Obtaining the required data for cluster CMD construction

As previously mentioned, for constructing a cluster CMD it is necessary to find out the colour index and apparent magnitude of each star member, as precisely as possible. Those values can be accurately obtained from photometric measurements derived from CCD images. However, those images must be *carefully processed* in order to assure that the derived data is a faithful representation of the real world.

a) Data Reduction

Before attempting any photometry measurement, the CCD stellar images (generically called “science” images, as they contain *scientific* useful data) have to be “normalized”. This normalization task refers to the elimination (or at least, to its maximal reduction) of the noise that both the CCD camera and the overall optical system has certainly introduced *per se* in the resulting science images.

In the case of CCD professional cameras, which operate at very low temperatures, the main causes of noise come from non-uniform responses from pixels and electronics. The optical system also introduces noise due to non-uniform responses from optical irregularities or randomly distributed dirties.

The electronic noise introduced by the CCD camera can be easily removed from any image by subtracting a *bias frame*, that is, an exposure of “zero duration” taken with the camera shutter closed. This special frame represents the *zero-point* or *base-line signal* from the CCD camera [4].

All the non-uniform responses, from both CCD and optical system, can be eliminated from any image by dividing it by a *flat field*, that is, an image of a perfectly even illuminated field. Any feature appearing in this special frame represents distortions introduced by the proper imaging system.

As the use of each different filter actually means a different overall optical system (each filter has its own irregularities), *a flat field for each filter must be obtained*.

Therefore, any image must undergo a two-stage process prior to any other action: firstly, the *bias frame* has to be subtracted; secondly, the resulted image has to be divided by the corresponding *flat field*.

It is highly recommended to average a set of many bias frames, in order to obtain a *master bias* that will result uncontaminated by any possible transitory effect (as the frequent appearing of *cosmic rays*). Usually, at least five bias are combined to obtain the *master bias*. In a similar manner, many flat fields of the same filter should be combined to assure the achievement of a more “representative” *master flat* for that filter.

b) Aperture photometry

Having the science images been reduced, any specific imaging processing software can be applied in order to obtain photometry values for each desired star. This is automatically performed by means of a procedure called *aperture photometry*. It consists in the following steps [5]:

1. The operator establishes the radius in pixels (the “aperture”) of a region, centered in the star, thought to contain almost all its light.
2. The operator establishes the inner and outer radii in pixels (the “annulus”) of a region, centered in the star, thought to contain no starlight at all, just “background”.
3. The operator selects an approximate center of the star image.
4. The program computes the exact centroid of the star image.
5. The program determines which pixels lie within the aperture, sums their counts, and computes the average pixel value in the aperture.
6. The program determines which pixels lie within the annulus, sums their counts, and computes the average pixel value in the annulus.
7. The program subtracts the average pixel value in the annulus from the average pixel value in the aperture, and gives a final *photometric value*.

The obtained *photometric values* are measurements of the counts from pixels only belonging to any considered star. This process permits to obtain *raw instrumental magnitudes*, that is, just *comparative* magnitude values that has not been yet corrected for the particular characteristics of the used telescope and CCD detector that captured the measured images, nor for the particular atmospheric absorption at the time of each image.

In order to select an optimum radius aperture, that is, one that provides the best signal-to-noise measurement, it is recommendable to previously analyze the *photometric curve of growth*. This is a graph that shows how the raw instrumental magnitude of a star varies with changes of the radius aperture used to determine it. The graph usually starts out low and rises to a plateau¹. The aperture should be selected balancing between a larger value (which assures that no starlight will be missed) and a lower one (which assures the lesser possible measurement errors due to the background contribution) [6].

c) Standardization

In order to find out *objective* stellar apparent magnitudes, that is, a *standard system*, it is necessary to transform the obtained raw instrumental magnitudes, eliminating all the particularities of the measurement process. As said, this implies to consider the distortions introduced by the proper imaging system and by the atmosphere as well.

Therefore, the equations to be resolved² are [7]:

$$m_B = B + x_1(B) + x_2(B) * (B - R) + x_3(B)*X(B) \quad (3)$$

$$m_R = R + x_1(R) + x_2(R) * (B - R) + x_3(R)*X(R) \quad (4)$$

¹ For good photometry results, the plateau region of the curve of growth should achieve an almost constant value (variation lesser than ± 0.05 magnitudes) [6].

² The particular case to be analyzed is for transforming instrumental magnitudes m_B and m_R into standard magnitudes B and R, but the equations are basically the same for whatever other pair of used filters.

where: m_B is the star's raw instrumental magnitude measured by the software on an image obtained through a standard B (blue) filter;
 m_R is the star's raw instrumental magnitude measured by the software on an image obtained through a standard R (red) filter;
 B is the star's true apparent magnitude measured through a standard B (blue) filter;
 R is the star's true apparent magnitude measured through a standard R (red) filter;
 $x_1(B)$ is the constant offset between the arbitrary assigned instrumental magnitudes and the corresponding standard magnitudes for the standard B (blue) wavelengths;
 $x_1(R)$ is the constant offset between the arbitrary assigned instrumental magnitudes and the corresponding standard magnitudes for the standard R (red) wavelengths;
 $x_2(B)$ is the blue color term introduced by the used optical system, which accounts for its particular response at standard B (blue) wavelengths;
 $x_2(R)$ is the red color term introduced by the used optical system, which accounts for its particular response at standard R (red) wavelengths;
 $x_3(B)$ is the blue airmass term, which accounts for the particular attenuation of the atmosphere regarding standard B wavelengths;
 $x_3(R)$ is the red airmass term, which accounts for the particular attenuation of the atmosphere regarding standard R wavelengths;
 $X(B)$ is the airmass at the moment of the obtained image through the standard B filter;
 $X(R)$ is the airmass at the moment of the obtained image through the standard R filter.

The usual way to resolve this system and find out the unknown terms is by also taking images of *reference stars lying as close as possible to the stars going to be studied*. Reference stars means stars of known apparent magnitude values accepted as standards by the astronomical community. Those reference stars has been catalogued from high precision photometry works, such as those performed by Arlo Landolt or Arne Henden.

By far, the most used reference catalog is the one developed by Landolt, which not only employed the Johnson-Cousins colour system filters, but has become the "practical definition" for the UBVRI standard system, which waveband characteristics is shown in Figure 4. The *Landolt fields*, as have been generically called, are a series of star regions near the celestial equator with well known magnitudes in at least the B, V and often R bands [8].

Therefore, knowing m_B , m_R , B , R , $X(B)$, $X(R)$, and assuming also known both $x_3(B)$ and $x_3(R)$ ³, the system (3) and (4) becomes reduced to just four unknown terms: $x_1(B)$, $x_2(B)$, $x_1(R)$ and $x_2(R)$. Having at least four sets of values from measured standard stars (two through the blue filter and two through the red one), the system can be resolved. For instance, equations (3) and (4) can be rewritten as

$$m_B - B - 0.263 * X(B) = x_2(B) * (B - R) + x_1(B) \quad (5)$$

$$m_R - R - 0.159 * X(R) = x_2(R) * (B - R) + x_1(R) \quad (6)$$

For each measured standard star at B band, the known left side of the equation (5) can be plotted against its corresponding $(B - R)$ value. Therefore, for just the two minimum required data from the blue filter, it becomes possible to graphically obtain the unknown

³ They both are quite constant, being $x_3(B) = 0.263$ and $x_3(R) = 0.159$.

terms $x_2(B)$ and $x_1(B)$, which respectively happen to be the angular coefficient and the intercept value in the vertical axis of the line that joins them. Proceeding in a similar way with equation (6) it can be found out the terms $x_2(R)$ and $x_1(R)$.

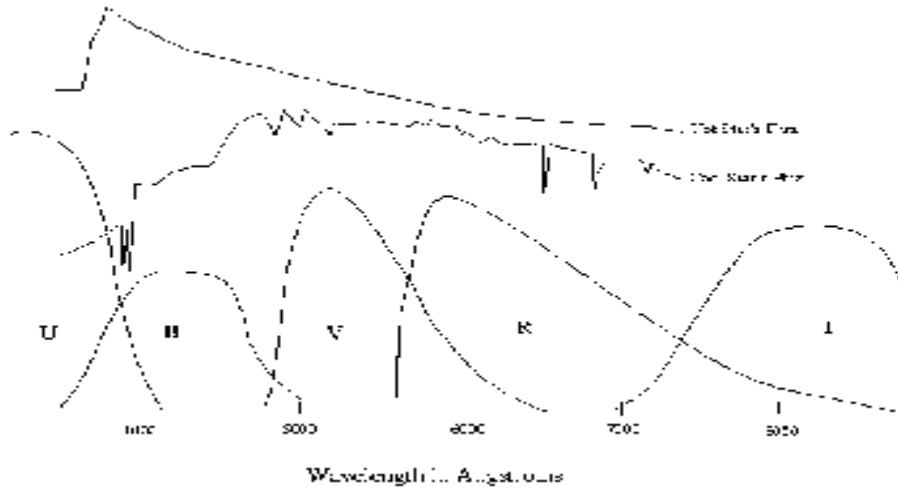


Figure 4
The UBVRI standard system bands

The final accuracy of the graphically obtained terms highly depends on the quality (*measurement precision*) of the measurements of m_B and m_R from the reference stars. It becomes quite obvious that by using as many as possible measurements from different reference stars instead of just the minimum required pair, term errors will be dramatically reduced.

Hence, the usual way is to find the correction terms is *by making a spread plot including all possible data*, and then use the least square linear solution. Their final accuracy can be estimated by computing the standard deviation and the median of the differences between reference (Landolt) values and the resulting values derived from just their application to *instrumental magnitudes*, that is those values obtained from:

$$B - R = \frac{m_B - m_R - [x_1(B) - x_1(R)] - [x_3(B) * X(B) - x_3(R) * X(R)]}{1 + x_2(B) - x_2(R)} \quad (7)$$

$$R = m_R - x_1(R) - x_2(R) * (B - R) - x_3(R) * X(R) \quad (8)$$

In particular, the standard deviations of the difference between the Landolt magnitudes and those derived from (7) and (8) will give the errors of the measurement.

Once all the “x” terms are known, and having been checked their correct accuracy, the *instrumental magnitude* of any star of the remaining science images can be properly converted into a *standard magnitude* by applying equations (7) and (8). Usually, the typical error in the conversion will be greater for faint objects than for bright ones.

4) The practical work

All the needed raw images for this project, including both sky and calibration frames, were supplied via Internet. Appendix 1 shows the complete list of provided images, all of them obtained from the McDonald Observatory in Texas, USA, and supplied without any further improvement process.

After all the images were uncompressed, they were ready to be processed by means of the application of the “AIP4WIN”⁴ software. All images were 2048 x 2048 pixels.

The first performed task was to cut overscan region off of all images, by applying the corresponding crop tool. All the images were cropped to 2045 x 2048 pixels.

Next, the image reduction process was executed according to:

- 1) **Bias correction:** The five supplied bias frames were averaged (the usual recommended process when the images to be combined are less than 7), resulting the *master bias*. This *master bias* was then immediately *subtracted* to each one of the rest of images (science and calibration), which became *bias corrected*.
- 2) **Master flats:** Each set of the five *flat field* images corresponding to the same filter were separately averaged, thus finally obtaining three independent *master flats*.
- 3) **Final reduction:** Each science bias corrected image was *divided by the master flat of the corresponding filter*.

Appendix 2 shows the *master bias*; Appendix 3, the *master flat B*; and Appendix 4, the final processed M67 R image.

Now all the science images were ready to *aperture photometry*. This application began by the supplied *Landolt field* images in order to find out the term corrections. All the photometry measurement was performed by applying “AIP4WIN” software.

First of all, it was necessary to identify each reference star by comparing the images to the corresponding Landolt reference celestial charts obtained from Internet [9]. As all the science images had the left and right sides mirrored compared to the Landolt reference celestial charts, it was necessary to perform a flop transformation in order to facilitate the identification of each reference star.

Next, after having been analyzed many *photometric curves of growth* for those particular science images, and also considered their overall stellar concentration, it was selected an aperture of 6.0 radius, and a sky annulus of 9.0 and 15.0 radius for its inner and outer dimensions. Arbitrary, the zero point constant was chosen as 20.0.

The instrumental magnitudes of the reference stars were then obtained. An excel worksheet (attached to this report) was constructed in order to gather all the information. The *Data Provided* page includes all the data corresponding to the reference field images.

⁴ “Astronomical Image Processing for Windows” is a program specifically designed for the case.

Each row represents each reference star, and the columns contain the star identification (column **A**), the used filter and its corresponding imaging time and airmass (columns **B**, **C** and **D** for the blue filter), the obtained instrumental magnitude (column **E** for the blue filter), the reference Landolt values (column **S** for the blue filter, column **V** for the colour index BR), the left side of equation (5) (column **AA**), the computation of BR from equation (7) (column **AP**), and the difference between the Landolt BR value and the obtained from equation (7) (column **AT**). Likewise, there are similar columns for data corresponding to the red and infrared filters.

With those values it was possible to resolve graphically equation (5) by plotting together columns **V** and **AA**, and equation (6) from columns **V** and **AE**. Some data (those appearing with blank row values) was specifically eliminated due to showing *great relative discrepancies with the rest of the sample* (that is, they laid notoriously apart than the overall tendency of the rest of data). Several reasons could explain such deviations (overexposure of the relative brighter stars, measurements performed to stars lying too close one from another, irregularities in the field images such as bad columns, etc).

Finally, the unknown terms became:

$$x_1(B) = -3.1098 \text{ and } x_2(B) = -0.0934 \quad (9)$$

$$x_1(R) = -1.873 \text{ and } x_2(R) = 0.0907 \quad (10)$$

Applying those correction terms to recalculate the standard magnitude values [equations (7) and (8)], resulted in median errors of -0.010 and 0.011 , and standard deviations of 0.082 and 0.072 , respectively for the colour index BR and the standard magnitude R. Being the medians lower than ± 0.08 , and standard deviations lower than 0.2 , the values for the correction terms proved to be satisfactory.

Next, it was done the same *aperture photometry* measurement to the stars of M67 contained inside a square area of 18 arcmin by side, centered in RA = 08h 51m 24.10s, DEC = $+11^\circ 48' 48''$ (J 2000.0), for both the B and R images. This area was arbitrarily chosen because it seemed to contain at least all the core of the cluster. The yellow square shown in Figure 5 represents such measured area.

The M67 B negative image was printed in order to allow the identification of each one of the stars inside the selected area. It was found 492 stars, many of them appearing very close from other stars, and a few even partially overlapping themselves.

The 492 stars from the M67 B image were attempted to be measured *in the same aperture photometry conditions as before*, followed by the same operation for the M67 R image. Many of the stars resulted unable to be measured, and even a few faint stars were simply “not found” in the M67 R image (probably due to introduced noise). Finally, 457 stars were actually measured from both B and R images.

Applying the same correction terms (9) and (10) to equations (7) and (8) it was obtained the corresponding M67 apparent magnitudes on a standard system. However, the resulting colour index BR values were not satisfactory, as all of them seemed to have been shifted to higher values. The origin of this problem is still unknown. A possible explanation would

be that the provided field images were not obtained by using the same equipment as the M67 images.

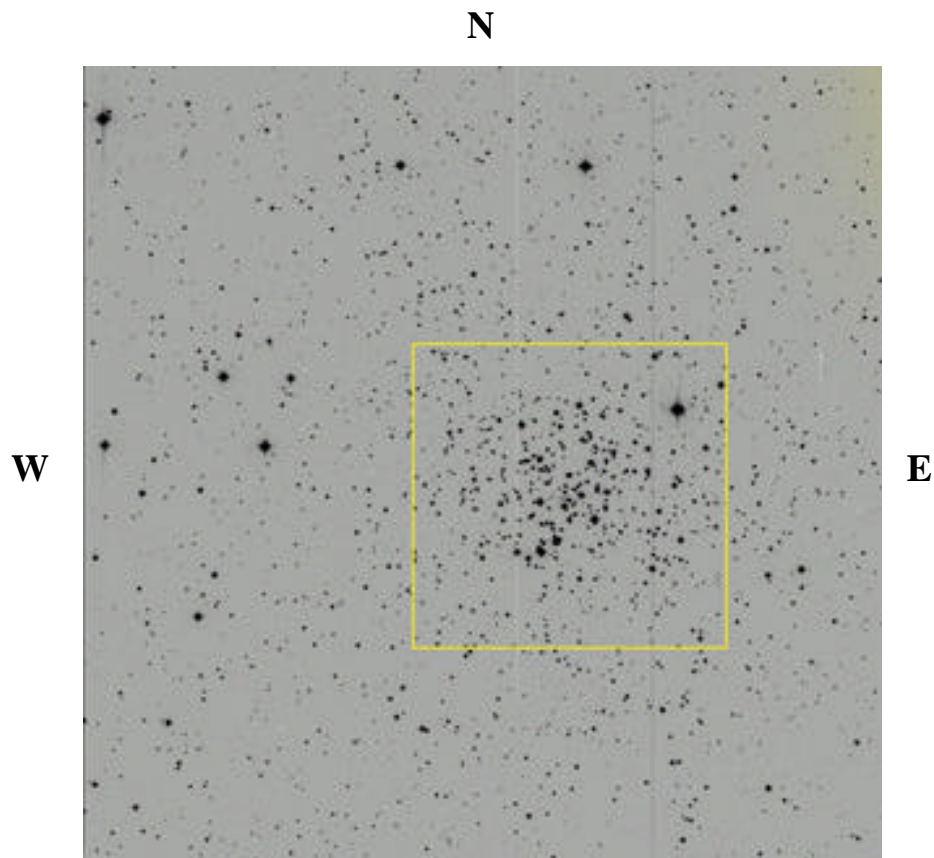


Figure 5
The measured area at the core of M67

The solution to overcome this difficult this was to obtain new correction terms from the very same M67 images, by applying the same procedure as before to a sample of stars of well known standard magnitudes. Luckily, it happens to be that there are several reference stars measured from M67 by Arne Henden, although its quantity -just 20 stars- is quite limited [10].

After having identified those 20 stars, their instrumental magnitudes was then obtained and collected in the spreadsheet at the *Observed* page, as well as all the corresponding data, in the same way as the *Data Provided* page. Data from the three brighter stars was finally not taken into account (they present noticeable deviations). From the remaining 17 reference stars the correction terms resulted:

$$x_1(B) = -2.0976 \text{ and } x_2(B) = -1.1819 \quad (11)$$

$$x_1(R) = -1.8287 \text{ and } x_2(R) = -0.7035 \quad (12)$$

As before, they were checked by computing medians and standard deviations (respectively 0.00 and 0.12 for the colour index BR, and -0.03 and 0.15 for the R standard magnitude).

The complete information for the surveyed stars of M67 (including data, measurements, and calculations performed with the latter correction terms) was collected in the *C-M Diagram* page of the same spreadsheet.

5) The obtained M67 CMD

From a spread plot of columns *M* and *N* of the *C-M Diagram* page, it was finally obtained the following M67 CMD:

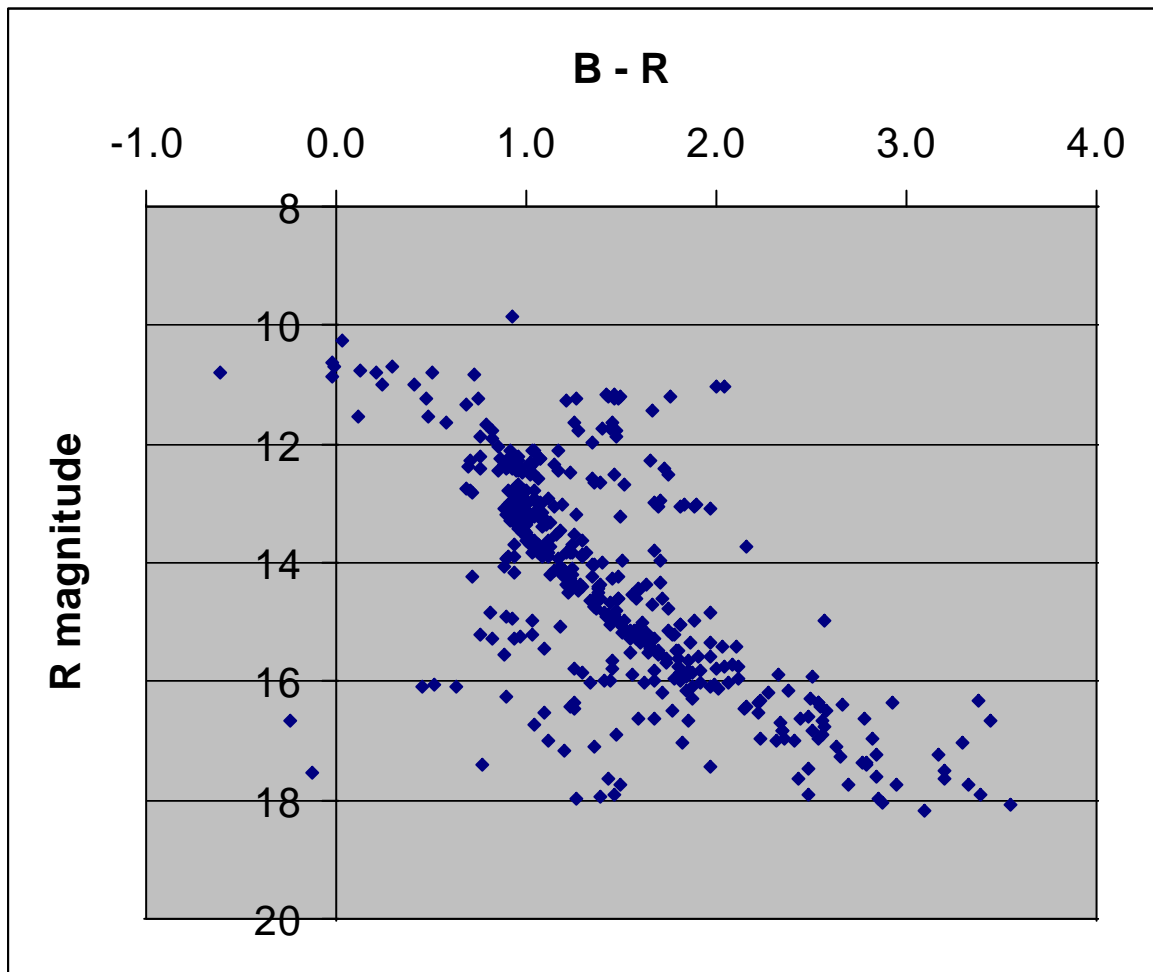


Figure 6
The obtained M67 colour-magnitude diagram

The data points that notoriously were “out of correspondence”, basically those laying lower than the 16th magnitude, and also those being below and to the left of the Main Sequence. The obvious explanation was that an important percentage of included data actually do not correspond to M67 stars.

Inside the measured area (324 arcmin^2) centered in M67 it was counted 492 stars, thus giving an image star density of $1.52 \text{ star/arcmin}^2$. As Figure 7 shows, the star counts for the same area at each corner of the M67 image gave 192, 261, 274, and 219 stars, although the two counts at the right side still seemed to be “contaminated” by the near presence of M67. For this reason, it can be considered a value of 206 stars (the average of the two left counts) as the image star average count for a 324 arcmin^2 area in the nearby region to M67 (giving an image star density of $0.63 \text{ star/arcmin}^2$).

Statistically arguing, this calculation implies that about 200 stars that appeared inside the yellow square actually do not belong to M67, being either foreground or background stars. As those “interloper” 200 stars (40 % of the sample) do not lay at the same distance as the truly cluster stars, their locations in the M67 CMD became spread following unknown patterns (although basically displaced in the vertical orientation, each shift actually depending on the true distance of the considered star).

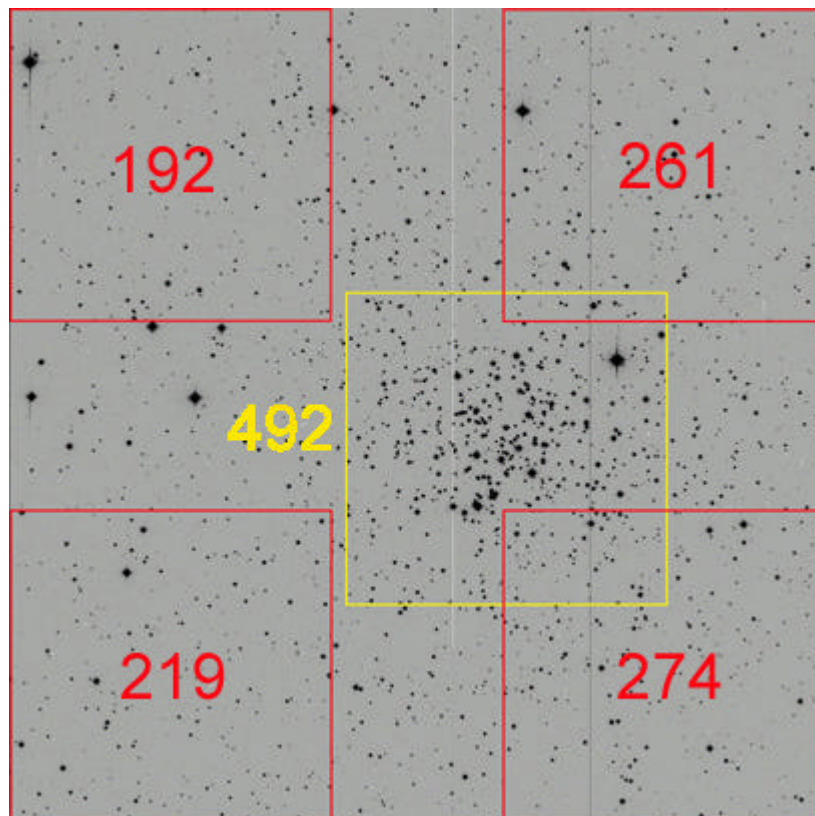


Figure 7
The star count for the same area in five different sectors

Another source of data error was possible due to the fact that the core of M67 is a very crowded area, which implied greater inaccuracies in the performed *aperture photometry*. (specially regarding that the applied “AIP4WIN” may not be *the best tool for the job*).

Having done the previous observations, the obtained M67 CMD was “cleaned” up to its most fundamental form, shown in Figure 8. In this basic sketch clearly appeared the Main Sequence, the Red Giant Branch, and the “golden” final objective: the turn-off point location (roughly estimated on standard magnitude $R = 13$, colour index $BR = 0.9$).

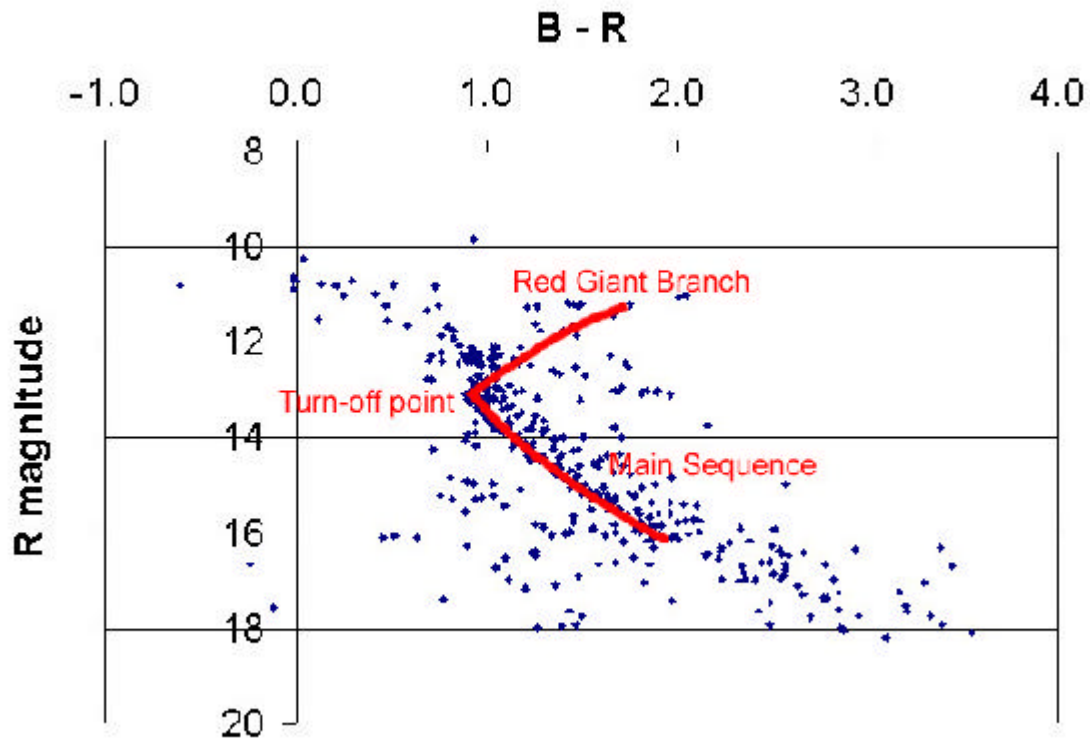


Figure 8
A schematic simplification of the M67 CMD of Figure 6

Now the road was all clear to determine M67's age and distance.

6) Deriving the age and distance to M67

The short length of Main Sequence in the M67 CMD announced that this open cluster is very old indeed. The age estimation came derived from the turn-off point location.

The sketched M67 CMD was overlapped to a similar Main Sequence CMD but plotted in absolute magnitudes⁵, both in the same scale (each vertical increment corresponded to the same magnitude variation for both graphs) as shown in Figure 9.

As mentioned at the theoretical description of this procedure, a well done fitting would have implied that not only the short M67 Main Sequence perfectly matched the long general Main Sequence plot, but also *for the same corresponding colour indexes*. As this

⁵ It was applied the CMD shown at the right side of Figure 3.

double condition turned out impossible to achieve simultaneously, the Main Sequence coincidence was priority considered.

Such found impossibility suggested *some problem with the obtained colour index values* (perhaps some offset was unnoticed introduced). The fact that the M67 CMD was expressed in colour index BR while the Main Sequence CMD was in colour index BV_0 , certainly introduced some error, but not enough to justify such difference. The BV_0 scale had to be expanded up to a factor of 1.7 in order to allow the proper fitting of the Main Sequence portions.

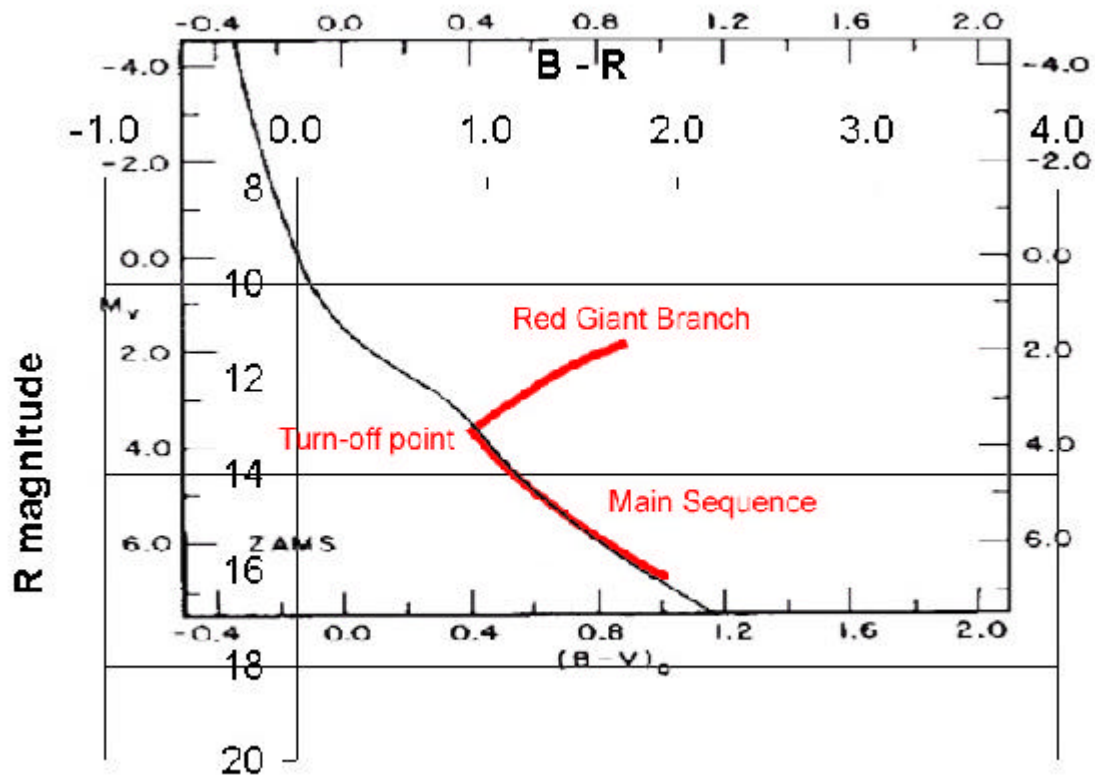


Figure 9

The sketched M67 CMD overlapped to the sketched MS CMD shown in Figure 3

Finally, the best fitting for the Main Sequence overall shape gave for the M67 turn-off point an absolute magnitude of 3.5.

This 3.5 result, applied to the Van den Berg's isochrones shown in Figure 2, converted it to an estimated age of 4,000 years for M67.

There are several intrinsic inaccuracies associated to this found age. First of all, the difficult in determining the "exact" turn-off point; secondly, the achievement of the proper magnitude values for it; and finally, the translation -via *stellar isochrones*- to the final age.

Regarding the contaminated M67 CMD, the performed simplification to place the turn-off point, and the problem with the color index, it could be conservatively estimated an overall error not less than 50 %.

The age of M67 is currently known with relative great uncertainty (its published values varying from 3.2 billion years [11] up to 9.4 billion years [12])⁶. Hence, it could be said that the obtained age was acceptable.

As the best fitting between the Main Sequence diagram and the Main Sequence portion of the sketched M67 CMD had been achieved for a vertical displacement that leveled apparent magnitude values to absolute magnitude values plus a 9.5 offset, this number became M67's *distance modulus*, and the distance was obtained from (2)

$$d = 10^{\left(\frac{13.0-3.5+5}{5}\right)} = 794 \text{ parsecs} = 2,590 \text{ light years}$$

The error in the found distance was basically associated to the difficult in achieving a correct fitting of the M67 Main Sequence to the general CMD.

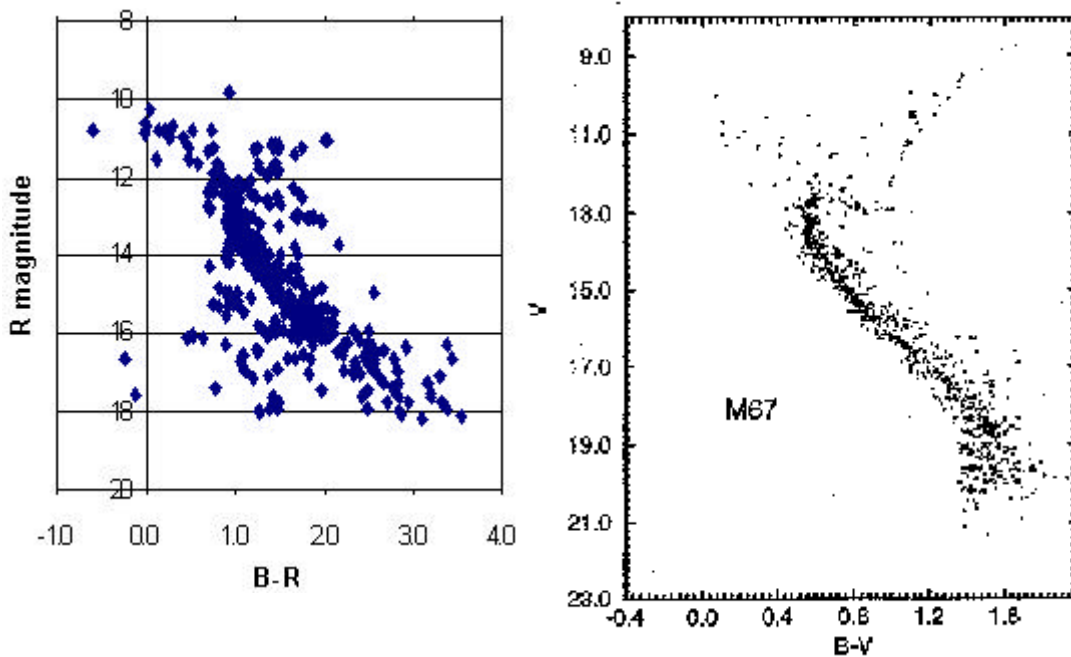


Figure 10
 A M67 CMDs comparison between the obtained and a published one

The best current M67's *distance modulus* is 9.7 (Dinescu, 1995) [13], so the found value is *amazingly good* (difference 2%), considering that (a) it has been derived by a comparative method which implies difficulties in finding the best fit; (b) the M67 CMD has been

⁶ This explains the eagerness of Dr. John Joseph Bochanski Jr. for using the Hubble Space Telescope to construct a new M67 CMD [3].

obtained from a highly contaminated sample of interloper stars; and (c) the M67 CMD plots apparent magnitudes at R band, instead of apparent magnitudes at V band.

A head to head comparison between the obtained M67 CMD and a published M67 CMD is shown in Figure 10. They have been respectively placed in order to have the same vertical scale (although the first is for R magnitudes, and the latter for V magnitudes). The comparison shows the correctness of the found Main Sequence shape and turn-off point magnitude, although the index colour, as said, does not coincide (it respectively corresponds to $BR = 0.9$ and $BV = 0.6$).

The obtained Main Sequence appears notoriously broadened, while the Red Giant Branch almost coincide up to magnitude 11. The left CMD gets very fuzzy down the 16th magnitude, and this is due to the already mentioned interloper “contamination”. Some stars that seem to “continue” the Main Sequence (up and to the left) may be *blue-straggler*, although this area must be necessarily so contaminated as the rest.

More accurate results would have been obtained if all surveyed stars were positively members of the cluster. This condition would allow a “clear” CMD, and hence a lesser uncertainty in the correct determination of the Main Sequence shape and turn-off location. The practical way to perform a “clear” cluster CMD would be to identify each star inside the field and delete all data corresponding to foreground or background stars.

Conclusion

Star clusters are the key to enter into the world of *stellar evolution*. The membership condition that all those stars share -being born at the same time from the same origin, and still remaining together, that is, laying at the same distance from us-, make them *the place* to look for development, confirmation or rejection about any theoretical conception about stellar evolution.

CMDs are the proper tool to analyze data from clusters. They achieve, at the same time, two fundamental properties: (1) they are quite simple to construct, just derived from photometric data; (2) they can supply a lot of important information.

From CCD images it is possible to obtain accurate photometric data. But such CCD raw information must be precisely processed in order to really become quality data. This implies not only to correct all possible introduced noise, but to make data independent of measurement particularities from both equipment and atmosphere as well.

As a practical exercise, it was constructed the CMD for the cluster M67 from provided images via Internet. The final diagram allowed the estimation of both its age and distance, achieving satisfactory results. This confirmed the tremendous potentiality of cluster CMDs, becoming a high recommendable investment considering time and resources consumption versus the essence of the deduced information.

References

- [1] “Measuring a Globular Star Cluster’s Distance and Age” by ESA, The ESA/ESO Astronomy Exercise Series 4, 2001, page 6
- [2] “Universe: Stars and Galaxies” by Roger A. Freedman and William J. Kaufmann III, R.R. Donnelley et Sons Company, 6 ed, 2002, page 481
- [3] “Determining the Age of the Old Open Cluster M67” by Dr. John Joseph Bochanski Jr., page 1, at <http://www.astro.washington.edu/stinson/HST/boo.pdf>
- [4] “Use of CCD Cameras” by SAO, CD-ROM HET 609 (Module 8, Activity 2), 2004
- [5] “The Handbook of Astronomical Image Processing” by Richard Berry & James Burnell, Willmann-Bell, Inc., 2000, pages 257-259
- [6] “Handbook of CCD Astronomy” by Steve B. Howell, Cambridge University Press, 2000, page 89
- [7] “Standard Calibrations” by Pamela Gay, page 9, at <http://stryder.fas.harvard.edu/ExcerptChptr2.pdf>
- [8] “A Practical Guide to Lightcurve Photometry and Analysis” by Brian D. Warner, Bdw Publishing, 2003, page 23
- [9] “UBVRI photometric standard stars in the magnitude range 11.5-16.0 around the celestial equator” by Arlo U. Landolt, Astronomical Journal 104, 1992, pages 340-371
- [10] “Arne Henden M67 file”, at <ftp://ftp.nofs.navy.mil/pub/outgoing/aah/m67>
- [11] “Companion - SkyAtlas 2000.0” by Robert A Strong and Roger W Sinnott, 2ed, Cambridge University Press, 2000, page 54
- [12] “WEBDA’s Cluster page for M67” by Jean-Claude Mermilloid, at http://obswww.unige.ch/webda/cgi-bin/ocl_page.cgi?dirname=ngc2682
- [13] “Determining the Age of the Old Open Cluster M67” by Dr. John Joseph Bochanski Jr., page 3, at <http://www.astro.washington.edu/stinson/HST/boo.pdf>

All images for this project have been provided from:

<http://astronomy.swin.edu.au/sao/students/projects/PamelaGay/>

Figures:

- 1 - “Star clusters” at <http://zebu.uoregon.edu/~js/ast122/lectures/lec12.html>
- 2 - <http://orca.phys.uvic.ca/astrocourses/a120/A120/lab5.html>
- 3 - left: <http://orca.phys.uvic.ca/astrocourses/a120/A120/lab5.html> ; right: “Ages and Distances of Clusters” at <http://www.physics.sfasu.edu/markworth/ast105/09agdist.htm>
- 4 - <http://orca.phys.uvic.ca/astrocourses/a120/A120/lab5.html>
- 5 - by the author
- 6 - by the author
- 7 - by the author
- 8 - by the author
- 9 - by the author
- 10 - left: by the author; right: <http://orca.phys.uvic.ca/astrocourses/a120/A120/lab5.html>

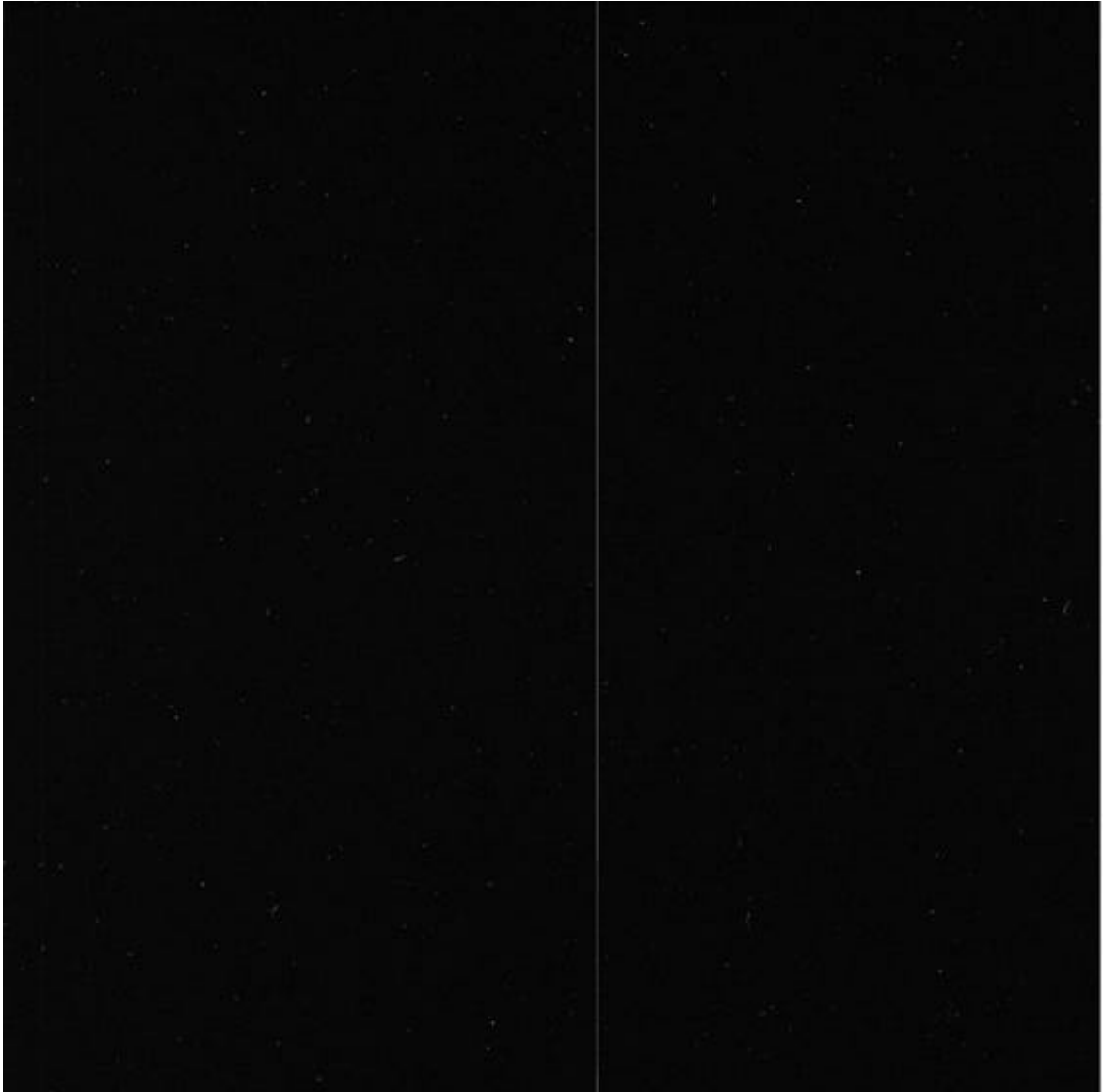
Appendix 1

The provided images from Internet

<i>Image code</i>	<i>Image</i>	<i>Date and UT time</i>	<i>Airmass</i>
Swin81_0001	B flat	2001-04-26 08:32	
Swin81_0002	B flat	2001-04-26 08:33	
Swin81_0003	B flat	2001-04-26 08:34	
Swin81_0004	B flat	2001-04-26 08:35	
Swin81_0005	B flat	2001-04-26 08:35	
Swin81_0006	R flat	2001-04-26 08:44	
Swin81_0007	R flat	2001-04-26 08:45	
Swin81_0008	R flat	2001-04-26 08:46	
Swin81_0009	R flat	2001-04-26 08:47	
Swin81_0010	R flat	2001-04-26 08:47	
Swin81_0011	I flat	2001-04-26 08:56	
Swin81_0012	I flat	2001-04-26 08:57	
Swin81_0013	I flat	2001-04-26 08:58	
Swin81_0014	I flat	2001-04-26 08:59	
Swin81_0015	I flat	2001-04-26 09:00	
Swin81_0022	SA 104 R	2001-04-24 03:04	1.087
Swin81_0023	SA 104 B	2001-04-24 03:09	1.083
Swin81_0024	SA 104 I	2001-04-24 03:14	1.078
Swin81_0025	M67 R	2001-04-24 03:21	1.073
Swin81_0026	M67 B	2001-04-24 03:27	1.071
Swin81_0027	M67 I	2001-04-24 03:32	1.069
Swin81_0028	NGC 4147 R	2001-04-24 03:38	1.075
Swin81_0029	NGC 4147 B	2001-04-24 03:44	
Swin81_0030	NGC 4147 B	2001-04-24 03:49	1.058
Swin81_0031	NGC 4147 I	2001-04-24 03:58	1.051
Swin81_0032	SA 104 R	2001-04-24 04:11	1.089
Swin81_0033	SA 104 B	2001-04-24 04:16	1.095
Swin81_0034	SA 104 I	2001-04-24 04:22	1.106
Swin81_0035	NGC 4147 R	2001-04-24 05:44	1.042
Swin81_0036	NGC 4147 B	2001-04-24 05:48	1.047
Swin81_0037	NGC 4147 I	2001-04-24 05:56	1.055
Swin81_0038	SA 107 R	2001-04-24 06:06	1.417
Swin81_0039	SA 107 B	2001-04-24 06:11	1.396
Swin81_0040	SA 107 I	2001-04-24 06:16	1.375
Swin81_0041	SA 107 R	2001-04-24 06:53	1.266
Swin81_0042	SA 107 B	2001-04-24 06:57	1.255
Swin81_0043	SA 107 I	2001-04-24 07:03	1.244
Swin81_0047	SA 107 R	2001-04-24 08:26	1.166
Swin81_0048	SA 107 B	2001-04-24 08:30	1.166
Swin81_0049	SA 107 I	2001-04-24 08:36	1.167
Swin81_0056	Bias		
Swin81_0057	Bias		
Swin81_0058	Bias		
Swin81_0059	Bias		
Swin81_0060	Bias		

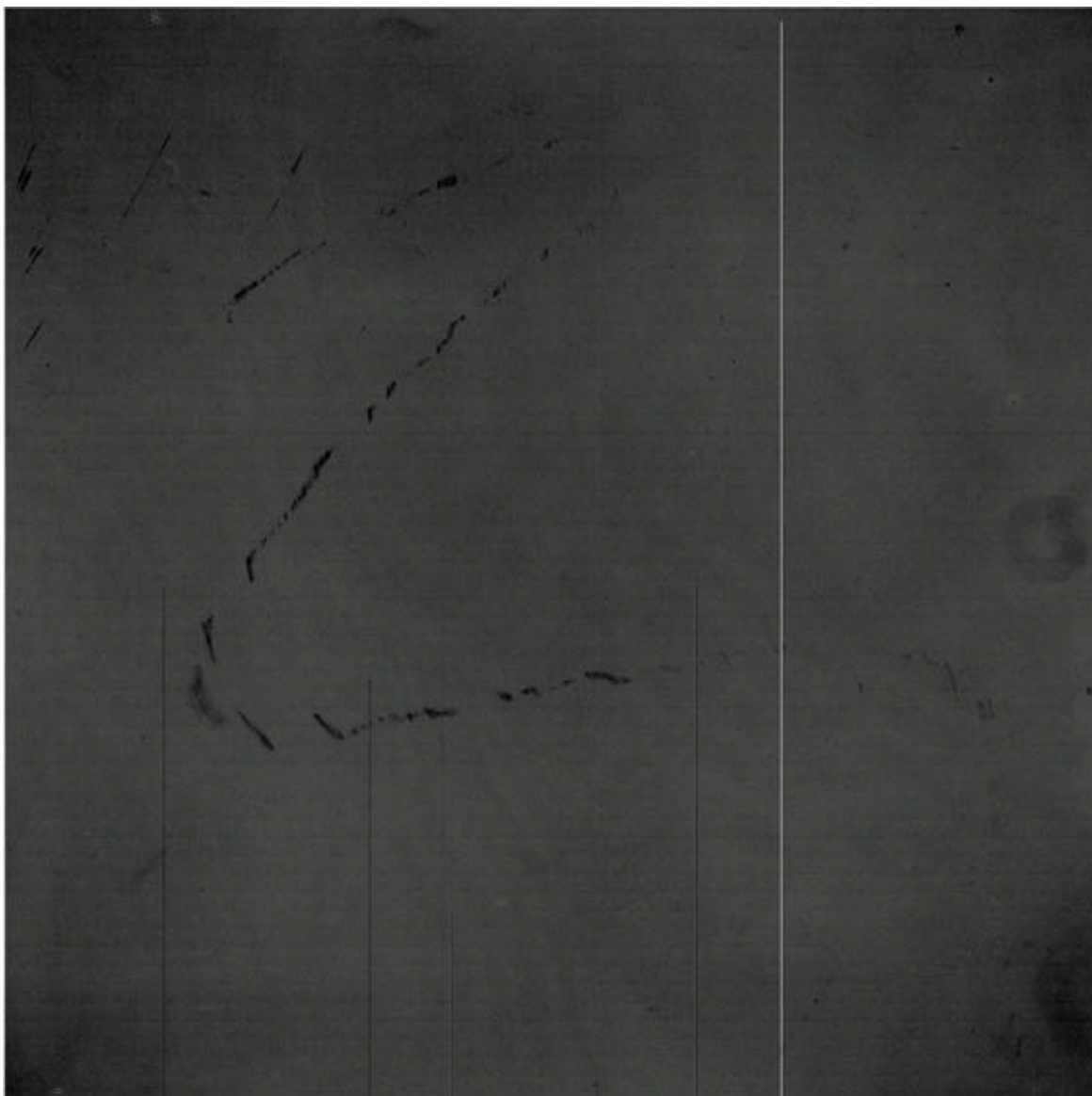
Appendix 2

The *master bias* image



Appendix 3

The *master flat B* image



Appendix 4

The M67 R final processed image

